

ELECTRICAL, OPTICAL AND STRUCTURAL PROPERTIES OF NANOSTRUCTURED Sb_2S_3 THIN FILMS DEPOSITED BY CBD TECHNIQUE

A.U. UBALE^{a*}, V.P. DESHPANDE^a, Y.P. SHINDE^a, D.P. GULWADE^b

^a*Thin Film Physics Laboratory, Department of Physics, Govt. Vidarbha Institute of Science and Humanities, Amravati, 444 604- INDIA*

^b*Department of Chemistry, Govt. Vidarbha Institute of Science and Humanities, Amravati, 444 604- INDIA*

Thin films of Sb_2S_3 were deposited onto glass substrate, by chemical bath deposition (CBD) method. The films were prepared in reaction bath at temperatures of 283, 303, 323 and 243 K by keeping deposition time constant. At elevated temperatures, the dissociation is greater and gives higher concentrations of Sb^{3+} and S^{2-} ions in reaction bath which enhances the deposition rate. The structure and surface morphology of the films were characterized by X-ray diffraction (XRD) and scanning electron microscopy (SEM). The films prepared shows transition from amorphous to polycrystalline nature depending on deposition temperature. The optical investigation showed that, films have direct allowed transitions in the range 1.86-2.30 eV depending on film thickness. The activation energy was found to decrease from 0.67 to 0.48 eV in low temperature and 0.19 to 0.09 eV in high temperature region with film thickness.

(Received January 16, 2010; accepted January 29, 2010)

Keywords: CBD, Sb_2S_3 , Nanostructured thin films, Electrical and optical properties.

1. Introduction

The electrical, optical and structural properties of nanostructured semiconductor thin films have attracted the attention of an increasing number of researchers from several disciplines in the last ten years. The size regime is exciting because it is where the transition from molecular to bulk behavior occurs. The nanophase semiconductors have their properties that are between molecule and bulk. Several investigators have prepared Sb_2S_3 thin films with different chemical methods such as spray pyrolysis [1-5], chemical bath deposition [6-8], successive ionic layer adsorption and reaction method [9], electrodeposition [10], dip and dry method [11] and vacuum evaporation [12-14]. The chemical bath deposition for formation of thin films from aqueous solution is a promising technique because of its simplicity and economics. The starting chemicals are universally available and inexpensive. This method can be used to deposit films at low temperature which avoids oxidation of the deposited material. The deposition conditions are easily controlled to get improved orientation and grain structure of the film [15]. The chemical bath deposition method has the major advantage with respect to other methods is that the films on different kinds of substrate shapes, and sizes can be deposited [16].

Antimony trisulphide is a significant binary chalcogenide due to extraordinary applications in the microwave devices [17], switching devices [18] and various optoelectronic devices [19-22]. In the present investigation films of Sb_2S_3 were prepared by CBD method using antimony potassium tartarate and sodium thiosulphate as antimony and sulphur source. Comparison of the structural, electrical, and optical properties of Sb_2S_3 films deposited at various deposition temperatures was discussed: in particular X-ray diffraction, electrical resistivity and optical absorption to observe the effect of the deposition temperature.

*Corresponding author: ashokuu@yahoo.com

2. Experimental details

2.1. Preparation of Sb₂S₃ thin films

Sb₂S₃ thin films were prepared onto glass substrate using chemical bath deposition by varying deposition temperature. The reaction bath for deposition contains 0.2 M 80 ml antimony potassium tartarate, 0.25 M 20 ml sodium thiosulphate and 0.1 M 40 ml tartaric acid, which was used as complexing agent. For the preparation of the film in antimony potassium tartarate solution, tartaric acid was added to form the complex and stirred for few seconds and then sodium thiosulphate was added in it. The well cleaned glass substrates were immersed vertically at the center of the reaction bath in such a way that they did not touch the walls of the beaker. The deposition process is based on the slow release of Sb³⁺ and S²⁻ ions in the solution, which then condensed on the substrate. The reaction of the positive and negative ions takes place to form neutral atoms which are then precipitated out and deposited to form thin film. The films, which are light brown in colour, were removed from the bath after a 1h deposition time. By keeping deposition time constant to 1 hour films were prepared at different deposition temperatures in the range 283 to 343 K.

2.2. Characterization methods

The film thickness being one of the imperative parameters which affects the properties of the thin film is calculated in present investigation by weigh difference method called as gravimetric method. Thickness is defined as the distance perpendicular to the surface from a point on the boundary surface, through the film to the other boundary surface. The film thickness is related to mass, area and density of the material as,

$$t = m / A\rho \quad (1)$$

where, m is the mass of the film deposited on the substrate which covers area A cm² and ρ is density of the material in bulk form (for Sb₂S₃ $\rho = 6.20$ gm/cm³). The mass of the deposited film is measured with the help of sensitive microbalance.

The structural properties of Sb₂S₃ thin films have been analyzed by X-ray diffraction (XRD) using CuK α radiation of wavelength 0.154 nm with Philips 1710 diffractogram. The microstructure of the Sb₂S₃ thin films on glass substrate was studied by using a scanning electron microscope JSM 610. The optical absorption was studied by using UV-VIS-NIR spectrophotometer Hitachi 330. The dark electrical resistivity of Sb₂S₃ film was measured using two-point dc probe method. A silver paste is applied for good ohmic contact to Sb₂S₃ thin film. The area defined was 0.5 cm².

3. Results and discussion

In chemical bath deposition method the film growth is affected by the precipitate formation process in the solution. To achieve auspicious condition for the film growth the ionic product (IP) must exceed the solubility product (SP), (IP>SP) thus the formation of thin film on the substrate takes place by ion-by-ion condensation [23]. The complexing agent as a constituent of the bath eliminates spontaneous precipitation by slowing down the release of the metallic ions on dissociation, thereby resulting in slow precipitation of the compound. The low temperature deposition avoids oxidation or corrosion of metallic substrates. In chemical deposition process pinhole free and uniform thin films were obtained as the reaction mixture from which these are deposited for all time remains in touch with the substrates. The following chemical reaction for the formation of the films has been suggested:

In aqueous solution Na₂S₂O₃ dissociates as,



$\text{Na}_2\text{S}_2\text{O}_3$ is a reducing agent by virtue of half cell reaction,



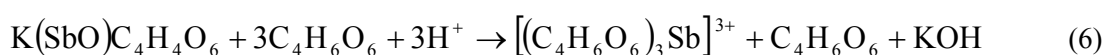
In acidic medium dissociation of $\text{S}_2\text{O}_3^{2-}$ takes place as,



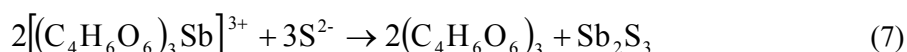
The electrons released in equation 2 react with S as,



The antimony potassium tartarate react with tartaric acid in acidic medium to give the complex with antimony as $[(\text{C}_4\text{H}_6\text{O}_6)_3\text{Sb}]^{3+}$,



The metal ion concentration and hence the rate of Sb_2S_3 formation in the solution was controlled by this complex. The metal ion concentration decreases with increase in complexing ions; consequently the precipitation rate is reduced and hence leading to terminal thickness.



Similar reaction mechanism was proposed by several workers for deposition of Sb_2S_3 films [24].

Figure 1 shows the deposition temperature dependence of the film thickness. The rate of deposition increases with temperature. At 283 K, the rate of film growth is slow (1.33 nm/min) and terminal film thickness of 80nm attained after 1h. However, at 343 K the growth rate is higher (4.55nm/min) and a terminal film thickness of 273 nm is attained after a period of 1h. The kinetic energy of the ions released at higher temperature is higher which increases the probability of interaction between them and the resulting condensation at the substrate surface [25]. Also increase in deposition temperature may increase the KE of the ions, that enhances dissociation

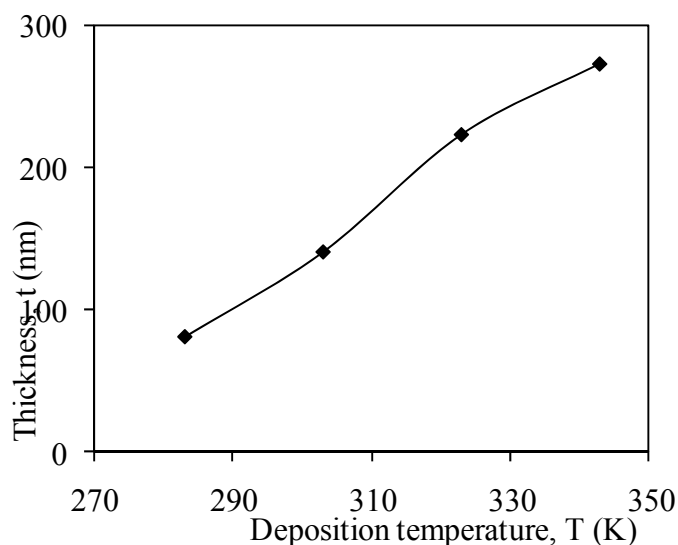


Fig. 1. Variation of Sb_2S_3 film thickness with deposition temperature (deposition time 1h).

The crystalline quality and orientation of the Sb_2S_3 films were investigated by X-ray diffraction. Figure 2 depicts the variation of the diffraction patterns of Sb_2S_3 films as a function of the deposition temperatures. The XRD patterns of film deposited at low temperature did not show any sharp peak. The consequences of X-ray diffraction show that with increasing the substrate temperature, the film structure transforms from amorphous to crystalline at the same deposition time.

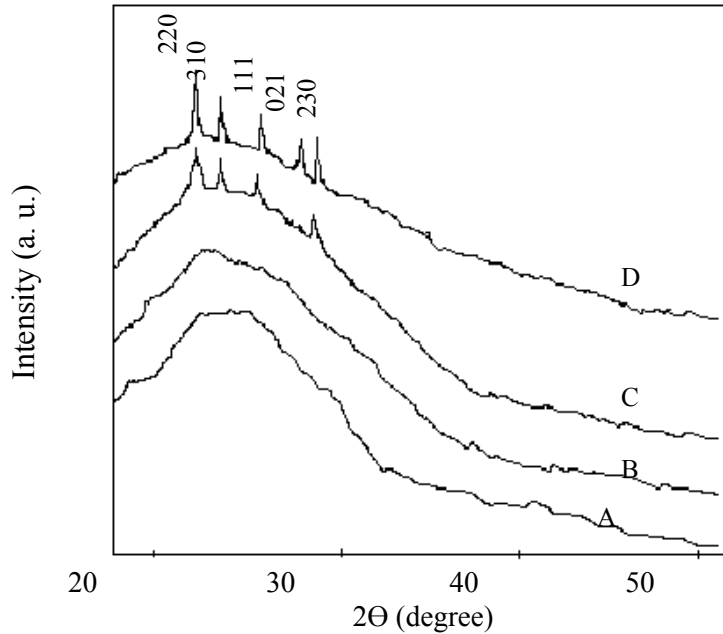


Fig. 2. XRD pattern of Sb_2S_3 thin films deposited at various temperatures: (A) 283 K, (B) 303 K, (C) 323 K, (D) 343 K.

The broad hump in XRD is due to amorphous glass substrate. As deposition temperature increases XRD pattern shows improvement in crystallite size. The intensity of the peaks increases with the deposition temperature of the film. The observed, d , values were compared with standard values, which confirm orthorhombic nature of Sb_2S_3 (Table) [26, 27]. The existence of the characteristic diffraction lines corresponding to the (2 2 0), (3 1 0), (1 1 1), (0 2 1) and (230) planes for Sb_2S_3 are clearly shown in the Figure 2. The average crystallite size of Sb_2S_3 film was calculated using Scherrer formula for plane (220),

$$d = \frac{\lambda}{\beta \cos \theta} \quad (8)$$

Where λ is the wavelength used (0.154 nm), β is the angular line width at half maximum intensity in radians and θ is the Bragg's angle. The grain size of Sb_2S_3 thin films was found 7 nm and 12 nm for the film deposited at 323 and 343 K temperature, which indicates significant improvement in crystallite size. The rise in the intensity of the peaks may be ascribed to grain enlargement related with larger thicknesses and increase in the degree of crystallinity by increasing the deposition temperature.

Table 1. Comparison of XRD data for Sb_2S_3 films deposited at various temperatures.

| Standard data ASTM Card 6-0474 | | Observed d values for Sb_2S_3 film (\AA^0) | | | |
|-----------------------------------|-------|---|----------------------|----------------------|----------------------|
| d (\AA^0) | h k l | Thickness 80(nm) | Thickness 140(nm) | Thickness 223(nm) | Thickness 273(nm) |
| 3.980 | 2 2 0 | - | - | 3.974 | 3.940 |
| 3.556 | 3 1 0 | - | - | 3.542 | 3.547 |
| 3.440 | 1 1 1 | - | - | 3.456 | 3.470 |
| 3.178 | 0 2 1 | - | - | - | 3.181 |
| 3.128 | 2 3 0 | - | - | 3.130 | 3.118 |

The surface images of Sb_2S_3 thin films deposited at 283 and 323 K temperature is shown in Figure 3. A lot of empty space is observed within these clusters. The cluster size shows remarkable rise with deposition temperature which confirms improvement in grain size.

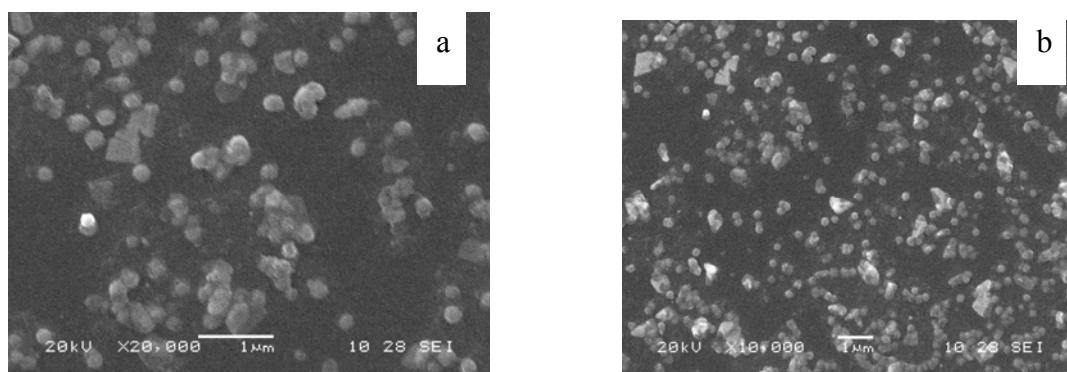


Fig 3. SEM images of Sb_2S_3 thin films deposited at different temperature: (a) 283 K and (b) 323 K.

The optical absorption studies have guide to a variety of interesting thin film optical phenomena which have thrown considerable light on the electronic structure of solids [28].

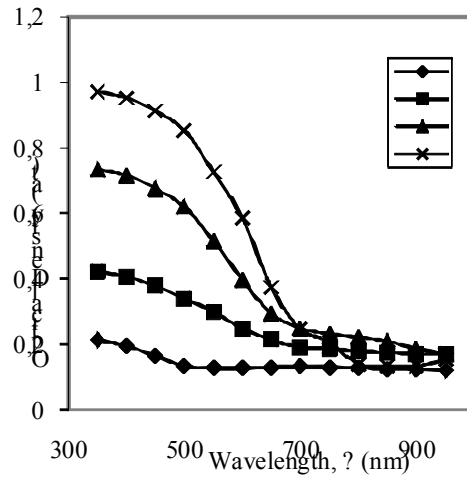


Fig. 4. Plot of optical density (αt) vs. wavelength for Sb_2S_3 films with different thickness: (A) 80 nm, (B) 140 nm, (C) 223 nm, (D) 273 nm.

The optical properties of a thin film usually are different from those of the bulk. The optical absorption of Sb_2S_3 thin films was studied in the wavelength range 300 to 1000 nm and the variation of optical density (αt) with wavelength (λ) is shown in the Figure 4. The absorption spectra of Sb_2S_3 films were analyzed using the classical relation,

$$\alpha = \frac{A(h\nu - E_g)^n}{h\nu} \quad (9)$$

where $h\nu$ is the photon energy, E_g is the optical band gap energy, A is constant and $n = 1/2, 2$ for allowed direct and allowed indirect transitions, respectively. The plots of $(\alpha h\nu)^2$ versus $h\nu$ were shown in Figure 5 for Sb_2S_3 films.

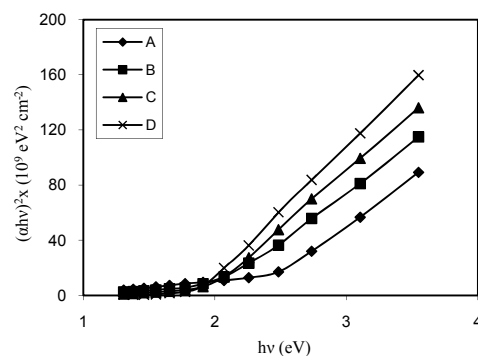


Fig. 5. Plot of $(\alpha h\nu)^2$ vs. $h\nu$ for film of thickness: (A) 80 nm, (B) 140 nm, (C) 223 nm, (D) 273 nm.

The value of E_g was changed from 1.86 to 2.30 eV as thickness of film varies from 273 to 80 nm (Figure 6). The decrease in band gap energy may be due to enhancement in the crystal properties. Due to smaller thickness certain size effects like quantum size effect may arise in the film [29]. In the energy spectrum as a consequence of quantization, the bottom of the conduction and top of the valence band may be separated by additional amount depending on thickness. The uppermost occupied valence band and lowest occupied conduction band are shifted to more negative and positive values respectively resulting in broaden of the band gap. This implies that the effective band gap energy of nanostructured is more than its bulk value [30].

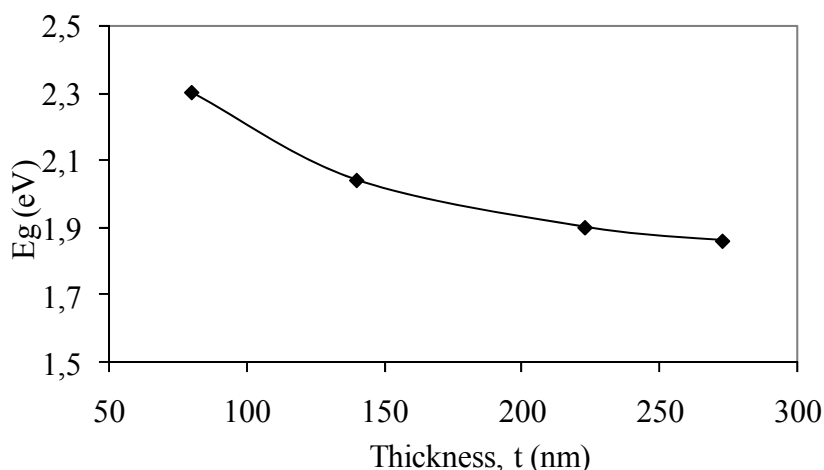


Fig. 6. Variation of optical band gap energy, E_g , with film thickness.

Fig. 7 shows the variation of the dark resistivity with temperature. It was observed that the resistivity of Sb_2S_3 thin films decreases with increase in temperature, indicating a semiconducting electrical behavior. The variation in electrical resistivity with film thickness implies (Figure 8) that when transport takes place through thin specimens the scattering of the charge carriers by the grain boundaries are more effective. This scattering may reduce the mobility below the bulk value showing high resistivity for the sample. It can be seen that the electrical resistivity decreases slowly with increasing temperature up to ~ 370 K then shows a sharp decrease with increasing temperature.

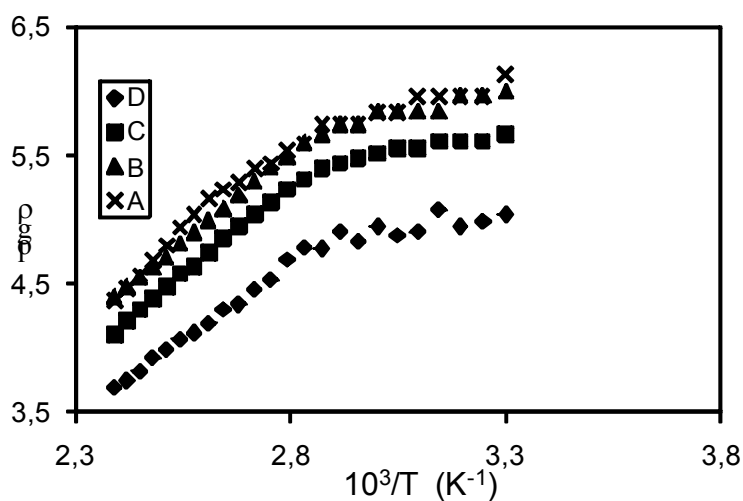


Fig. 7. Variation of $\log \rho$ vs. $10^3/T$ for Sb_2S_3 films with different thickness: (A) 80 nm, (B) 140 nm, (C) 223 nm, (D) 273 nm

The thermal activation energy was calculated using the relation,

$$\rho = \rho_0 \exp (E_0/KT) \quad (10)$$

where, ρ is resistivity at temperature T , ρ_0 is a constant, K is Boltzmann's constant and E_0 is the activation energy required for conduction. The activation energy is found to decrease from 0.67 to 0.48 eV in low temperature and 0.19 to 0.09 eV in high temperature region with increase in film thickness from 80 to 273 nm (Fig. 9).

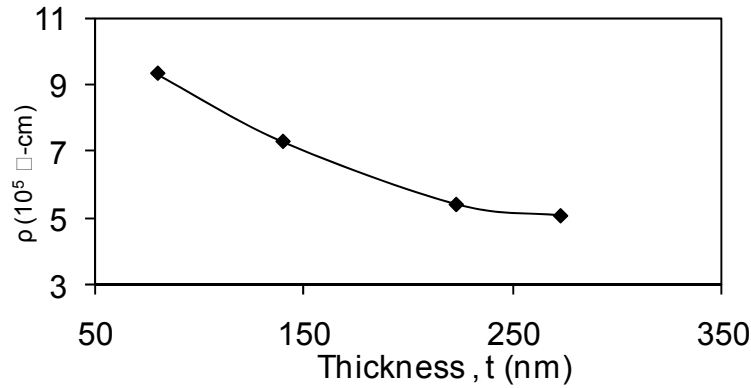


Fig. 8. Plot of variation of electrical resistivity, ρ , with thickness of Sb_2S_3 films at temperature 333 K.

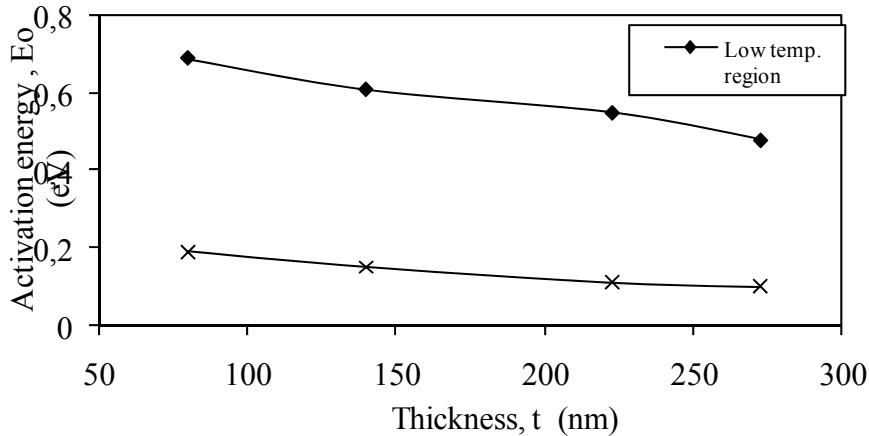


Fig. 9. Variation of activation energy, E_0 , with film thickness.

4. Conclusions

In conclusion, Sb_2S_3 thin films were prepared at room temperature from aqueous bath using chemical bath deposition method. The films at different deposition temperatures were prepared by keeping deposition time constant. The films prepared shows transition from amorphous to polycrystalline nature depending on deposition temperature. The optical investigation showed that Sb_2S_3 thin films have direct allowed transitions. The value of optical band gap energy increase from 1.86 to 2.30 eV as thickness of the film decreases from 273 to 80 nm. The activation energy is found to decrease from 0.67 to 0.48 eV in low temperature and 0.19 to 0.09 eV in high temperature region with increase in film thickness from 80 to 273 nm.

Acknowledgement

The authors are thankful to University Grants Commission, WRO, Pune (India), for financial support under the project (No: F47-258/2008).

References

- [1] K.Y. Rajpure, C. H. Bhosale and C.D. Lokhande, *Thin Solid Films*, **311**,114 (1997).
- [2] C.H. Bhosale, M.D. Uplane, P.S. Patil and C.D. Lokhande, *Thin Solid Films*, **248**, 137 (1994).
- [3] V.V. Killedar, C.D. Lokhande and C.H. Bhosale, *Mater. Chem. Phys.*, **47**,104 (1997).
- [4] K.Y. Rajpure, C.D. Lokhande and C.H. Bhosale, *Mater. Chem. Phys.*, **51**, 252(1997).
- [5] V.V. Killedar, C.D. Lokhande and C.H. Bhosale, *Indian J. Pure Appl. Phys.* ,**36** ,33 (1998).
- [6] R.S. Mane, B.R. Sankpal and C.D. Lokhande, *Thin Solid Films*, **353**, 29 (1999).
- [7] C.D. Lokhande, *Indian J. Pure Appl. Phys.*, **29**, 300 (1991).
- [8] J.D. Deasi and C.D. Lokhande, *Thin Solid Films*, **237**, 29 (1994).
- [9] B.R. Sankpal, H.M. Pathan and C.D. Lokhande, *J. Mater. Sci. Lett.*, **18**, 1453 (1999).
- [10] N.S. Yesugade, C.D. Lokhande and C.H. Bhosale, *Thin Solid Films*, **263**, 145 (1995) .
- [11] B.B. Nayak, H.N. Acharya, T.K. Choudhuri and G.B. Mitra, *Thin Solid Films*, **92**, 309 (1982).
- [12] I.K. El Zawawi, A. Abdel-Moez F.S., Terra M. Mounir, *Thin Solid Films* **324**, 300 (1998).
- [13] N. Tigau, C. Gheorgies, G.I. Rusu and S. Condurache-Bota, *J. Non-Cryst. Solids*, **351**, 987 (2005).
- [14] N. Tigau, *Cryst. Res. Technol.*, **42**, 281 (2007).
- [15] R.S. Mane and C.D. Lokhande, *Mater. Chem. Phys.*, **65**, 1 (2000).
- [16] O. Savadogo and K.C. Mandal, *J. Electrochem. Soc.*, **139** ,L16 (1992).
- [17] J. Grigas, J. Meshkanskas and Orlimas, *Phys. Stat. Solidi* ,(A) **37**, 10 (1976).
- [18] M.S. Ablowa, A.A. Andreev, T.T. Deb Akaev, B.T. Melekh, A.B. Peutsow, N.S. Sheridel and L.N. Shivilona, *Sov. Phys. Semicond.*, **10**, 29 (1976).
- [19] M.J. Chokalingam, K. Nagarajo Rao, R. Rangarajan and C.V.Suryanarayana, *J. Phys. D: Appl. Phys.*, **3**, 1641 (1970).
- [20] O. Savadogo, K.C. Mandal, *J. Electrochem. Soc.* **141**, 2871 (1994).
- [21] E. Montrimas , A. Pazera, *Thin Solid Films* **34**, 65 (1976).
- [22] J. George, M. K. Radhakrishanan, *Solid State Commun.* **33** ,987 (1980).
- [23] R.B. Barnes, M. Czeeny, *Phys. Rev.* **38**, 323 (1931).
- [24] O. Savadogo and K.C. Mandal, *Sol. Energ. Mater. Sol. Cell.*, **26**, 117 (1992).
- [25] R.C. Kainthla, D.K. Pandya and K.L. Chopra, *J. Electrochem. Soc.* ,**127** ,277(1980).
- [26] ASTM diffraction data file card no 6-0474.
- [27] C. D. Lokhande, *Mater. Chem. Phy.* ,**27**, 1 (1991).
- [28] K.L. Chopra, *Thin film Phenomena*, (McGraw-Hill, NewYork, 1969).
- [29] P.K. Nair, M.T.S. Nair, V.M. Garcia, O.L. Arenas, Y. Pena, A. Castillo, I.T. Ayala, O. Gomezdaza, A. Sanchez, J. Campos, H. Hu, R. Suarez and M.E. Rincon, *Sol. Energ. Mater. Sol. Cell.*, **52**, 313 (1998).
- [30] L.E. Brus, *Nanostruct. Mater.*, **1**, 71 (1992).